



Effect of Rosuvastatin on Myocardial Apoptosis in Hypertensive Rats Through SIRT1/NF- κ B Signaling Pathway

Xiangqian Ren, Yi Wang, Lin Han, Zhenzhen Sun, Bin Yuan*

Department of Cardiology, Anning Branch, 940 Hospital of the Joint Service support Force of the Chinese People's Liberation Army, Gansu, 730070, China

ARTICLE INFO

Original paper

Article history:

Received: January 11, 2022

Accepted: March 17, 2022

Published: April 30, 2022

Keywords:

rosuvastatin, SIRT1/NF- κ B signaling pathway, hypertensive rats, myocardial apoptosis

ABSTRACT

The study aimed to observe the effect of rosuvastatin on myocardial apoptosis in hypertensive rats through the silent information regulator 1 (SIRT1)/nuclear factor- κ B (NF- κ B) signaling pathway. The spontaneously hypertensive rat (SHR) model was established, and the rats were randomly divided into the SHR group, Rosuvastatin group and Control group. The blood pressure, creatine kinase (CK) and other myocardial indexes in each group were detected, the cardiac function indexes of rats were determined using magnetic resonance imaging (MRI) and echocardiography (ECG), and tumor necrosis factor- α (TNF- α) and interleukin-6 (IL-6) in myocardial tissues were detected via enzyme-linked immunosorbent assay (ELISA). Moreover, the apoptosis level of myocardial tissues was detected using terminal deoxynucleotidyl transferase-mediated dUTP nick end labeling (TUNEL) staining. Finally, the expression levels of the SIRT1/NF- κ B signaling pathway and apoptosis genes and proteins in myocardial tissues in each group were detected via quantitative polymerase chain reaction (qPCR) and Western blotting. In the SHR group, the blood pressure, the levels of serum creatinine (CR) and CK were increased ($p < 0.05$). In the SHR group, both fractional shortening (FS%) and ejection fraction (EF%) were obviously lower than those in the control group ($p < 0.05$), while both left ventricular end-diastolic diameter (LVEDd) and left ventricular end-systolic diameter (LVESd) were higher than those in the control group ($p < 0.05$), and the levels of TNF- α , IL-6 and myeloperoxidase (MPO) were increased ($p < 0.05$). The number of apoptotic cells in myocardial tissues in the SHR group was larger than that in the other two groups ($p < 0.05$). In the SHR group, the expression levels of Caspase3 and NF- κ B were remarkably higher than those in the Rosuvastatin group ($p < 0.05$), while the expression levels of Bcl-2 and SIRT1 were remarkably lower than those in the Rosuvastatin group ($p < 0.05$). Rosuvastatin can inhibit myocardial apoptosis in hypertensive rats through up-regulating SIRT1 and down-regulating NF- κ B.

DOI: <http://dx.doi.org/10.14715/cmb/2022.68.4.23>

Copyright: © 2022 by the C.M.B. Association. All rights reserved.



Introduction

Arterial hypertension has become a major health problem due to its high morbidity rate and cardiovascular risk accompanied, which has been identified as a major risk factor for cardiac death, seriously affecting the health and quality of life of patients (1). Hypertension refers to the increase in systolic arterial pressure or diastolic pressure ($\geq 140/90$ mmHg) in a resting state, which is the major cause of cardiomyopathy (2, 3). Human primary hypertension often leads to cardiac remodeling, ventricular hypertrophy and congestive heart failure (4) and causes cardiac dysfunction, further resulting in poor clinical prognosis, ultimately causing severe cardiovascular diseases (5). Cardiovascular diseases threaten the health and even cause death in the world.

The incidence rates of heart failure, arrhythmia and coronary heart disease in patients with hypertension are 8-10 times that in normal people (6). Therefore, exploring the pathogenesis of hypertension is of great significance in the prevention and treatment of cardiovascular diseases such as heart failure. However, the treatment strategies and pathogenesis of hypertensive cardiomyopathy have not been perfected yet. Currently, only several related factors have been discovered by researchers (7, 8). Myocardial hypertrophy and apoptosis are key pathological changes in cardiac dysfunction. It is reported that in the pathophysiological process, myocardial apoptosis is one of the causes of the decline in myocardial mass (9). However, the specific role of apoptosis in end-stage hypertensive heart disease remains unclear and

*Corresponding author. E-mail: yuhoicuo35838@163.com
Cellular and Molecular Biology, 2022, 68(4): 194-201

is poorly understood, and it is regulated by a variety of cell growth factors.

Silent information regulator 1 (SIRT1) plays an important role in cell homeostasis, and the SIRT1 signaling pathway is essential for the anti-apoptotic property in diseases (10). Recent studies have demonstrated that SIRT1 has an important role in DNA damage repair, inhibition of apoptosis, oxidative stress, etc. Under ischemic or hypoxic conditions, SIRT1 can deacetylate to enhance the resistance of cells to oxidative stress (11). Multiple signaling pathways are involved in the inflammatory response and tissue damage. Nuclear factor- κ B (NF- κ B) can control many biological processes, such as inflammation and apoptosis (12). A study has shown that NF- κ B can significantly promote the production of tumor necrosis factor- α (TNF- α), causing toxicity of TNF- α to the body (13). Therefore, the dysregulation of the NF- κ B signal transduction mechanism is a potential cause of various diseases (14). As an inflammatory switch or sensor, NF- κ B produces the inflammatory response to various stimuli and initiates inflammatory genes. The nuclear transcription factor can be activated by many factors, leading to the activation of NF- κ B (15). Therefore, it is important to understand the correlation between NF- κ B and various downstream signaling molecules. In the case of dysregulation, NF- κ B will be the driving force of diseases. However, the specific mechanism of the effect of the SIRT1/NF- κ B signaling pathway on hypertension and myocardial apoptosis remains unclear. In this experiment, therefore, the effects of the SIRT1/NF- κ B signaling pathway on myocardial apoptosis and inflammation in hypertension were verified using a variety of molecular methods, hoping to provide an experimental and theoretical basis for the prevention and treatment of myocardial apoptosis in hypertension through the SIRT1/NF- κ B signaling pathway.

The present study aims to explore the effect of rosuvastatin on myocardial apoptosis in hypertensive rats and its influence on the SIRT1/NF- κ B signaling pathway. In this study, the effect of rosuvastatin on myocardial apoptosis in hypertensive rats was clarified using *in vivo* experiments and various molecular biological techniques, the cardiac function indexes and pathway-related protein expressions were detected after intervention with rosuvastatin in the

hypertensive rat model, and the effect of rosuvastatin on myocardial apoptosis in rats through the SIRT1/NF- κ B pathway was determined, so as to provide important experimental support for the treatment of myocardial apoptosis in hypertension with rosuvastatin, as well as theoretical and experimental references for the subsequent research and development of new drugs for myocardial apoptosis in hypertensive rats.

Materials and methods

Commonly used reagents and consumables

TNF- α and interleukin-6 (IL-6) enzyme-linked immunosorbent assay (ELISA) kits (Nanjing Jiancheng Bioengineering Institute), TRIzol reagent, DEPC-treated water, SuperScript III RT kit and SYBR quantitative polymerase chain reaction (qPCR) Mix (ABI), RIPA lysis buffer (Beyotime), loading buffer, protease inhibitor and BCA protein concentration assay kit (Biosharp), β -actin and secondary antibodies (Boster Biological Technology Co., Ltd.), primary antibodies (Santa), tissue homogenizer and electrophoresis apparatus (Bio-Rad), microplate reader (Thermo), 2500 gel imager (Bio-Rad, USA), and qPCR instrument (7900 Fast, Applied Biosystems).

Animal modeling and grouping

Twenty male Wistar spontaneously hypertensive rats (SHRs) aged 8 weeks old and weighing about 250 g were randomly divided into the SHR group (n=10) and Rosuvastatin group (10 mg/kg/d, n=10) after adaptive feeding. Another 10 Wistar rats were used as the Control group. The experimental scheme was approved by the Laboratory Animal Ethics Committee, and all animal operations were performed in accordance with the regulations in the NIH Laboratory Animal Guide. The rats in each group were fed for 2 weeks. After the trial period, the blood and myocardial tissue samples were collected from rats in each group, and one portion of tissues was stored in 4% paraformaldehyde for hematoxylin-eosin (HE) staining and the other one was stored in a refrigerator at -80°C to detect the expression levels of genes and proteins.

The study was approved by the ethics committee of 940 Hospital of the Joint Service support Force of the Chinese People's Liberation Army

Detection of arterial blood pressure and myocardial function of rats

After the experiment, the systolic blood pressure and diastolic blood pressure (mmHg) of the caudal artery were measured using a sphygmomanometer in accordance with the instructions of the instrument. To predict the occurrence of myocardial apoptosis in hypertensive rats in clinical practice in advance and provide important references for early diagnosis, the myocardial function indexes creatine kinase (CK) and creatinine (CR) were detected. The blood was routinely drawn from rats in each group and centrifuged at 2000 g for 10 min under low temperature, and the serum separated was collected, followed by detection using a full-automatic biochemical analyzer.

Determination of cardiac physiological function indexes

To observe whether hypertension induces myocardial dysfunction, the left ventricular function was determined through magnetic resonance imaging (MRI) and echocardiography (ECG) under the transducer frequency of 10 MHz, including left ventricular end-diastolic diameter (LVEDd), left ventricular end systolic diameter (LVESd), ejection fraction (EF) and fractional shortening (FS), according to the instructions of the instrument.

Detection of inflammatory factors in each group

After the rats were anesthetized and sacrificed, the myocardial tissues were harvested and washed with normal saline. Then 0.5 g of myocardial tissues were taken, smashed using the homogenizer with tissue lysis buffer prepared already, and centrifuged at 1500 g for 15 min. Then the supernatant was collected to detect the changes in levels of myeloperoxidase (MPO), IL-6 and TNF- α . Finally, the absorbance of indexes in each group was detected using the microplate reader, and the standard curves were plotted, based on which the changes in content were analyzed according to the instructions.

HE staining

The rats were sacrificed via dislocation at one time, and the heart was isolated and fixed with 4% paraformaldehyde at 4°C for 48 h. The tissues were

washed with running water, dehydrated with ethanol at different concentrations and embedded in paraffin. Then they were routinely sliced into 4-5 μ m-thick sections, deparaffinized and hydrated with 95%, 90%, 80%, 75% and 50% ethanol. Finally, the pathological changes in myocardial tissues were observed under a light microscope.

Terminal deoxynucleotidyl transferase-mediated dUTP nick end labeling (TUNEL) apoptosis assay

The myocardial apoptosis of paraffin sections was detected using the TUNEL apoptosis assay kit (Roche), as follows: The tissues were fixed, rinsed, infiltrated with 0.1% Triton X-100 and prepared into paraffin sections, followed by labeling reaction of sealed sections using the fluorescence developer. The FITC-labeled TUNEL-positive cells were observed under a fluorescence microscope, and the TUNEL-positive cells were counted in 10 fields of view.

QRT-PCR

The total RNA was extracted using TRIzol (Invitrogen) from myocardial tissues and reversely transcribed into cDNA (the use of isopropanol was noted) after the RNA purity and concentration were detected qualified. The primer amplification was performed using the system (20 μ L): 2 μ L of cDNA, 10 μ L of the mix, 2 μ L of primers and 6 μ L of ddH₂O, for a total of 40 cycles. Then the PCR amplification was performed: pre-denaturation at 95°C for 2 min, 94°C for 20 s, 60°C for 20 s and 72°C for 30 s, for a total of 40 cycles. The primer sequences of target genes and the internal reference β -actin were designed according to those in the GenBank (Table 1). The expression levels of target genes were detected via qRT-PCR. The mRNA expression level in myocardial tissues in each group was calculated using $2^{-\Delta\Delta Ct}$.

Table 1. PCR primers used in this experiment

Target gene	Primer sequence
β -actin	F: 5'-CAGTGCCAGCCTCGTCTCAT-3' R: 5'-AGGGCCATCCACAGTCTTC-3'
Caspase3	F: 5'-CTACCGACCCGGTTACTAT-3' R: 5'-TTCCGGTTAACACGAGTGAG-3'
Bcl-2	F: 5'-GGTGTCTTGAGATCTCTGG-3' R: 5'-CCATCGATCTCAGAAGTCTC-3'
SIRT1	F: 5'-GCAACAGCATCTTGCCTGAT-3' R: 5'-GTGCTACTGGTCTCACTT-3'
NF- κ B	F: 5'-CTGAACAGGGCATACTGT-3' R: 5'-GAGAAGTCCATGTCCGCAAT-3'

Western blotting

The myocardial tissues were cut into pieces, weighed and added with RIPA lysis buffer (100 mg: 1 mL) for tissue homogenization. The protein was extracted, and the protein concentration was calculated using the BCA protein assay kit. Then Western blotting was performed: The gel was prepared for protein loading and electrophoresis, and the protein was transferred onto a membrane, sealed, incubated with the primary antibody overnight and incubated again with the secondary antibody for 1 h. The freshly prepared ECL mixture was added, and the color was developed in a darkroom. The protein band was scanned and quantified using the Odyssey scanner, and the level of protein to be detected was corrected using GAPDH. Finally, the Western blotting bands were quantified using Image Lab software. The protein expression in each group was calculated.

Statistical analysis

All raw data in the experiments were statistically analyzed using SPSS 20.0 software, and multiple comparisons were performed. The experimental results were expressed as mean \pm standard deviation ($\bar{x}\pm s$). $p < 0.05$ suggested that the difference was statistically significant. The bar graph was plotted using GraphPad Prism 7.0.

Results and discussion

Myocardial function and blood pressure

As shown in Table 2, both systolic blood pressure and diastolic blood pressure in the SHR group were significantly higher than those in the Control group ($p < 0.05$). According to the detection results of myocardial function indexes, the levels of serum CR and CK were significantly higher in the SHR group than those in the Control group ($p < 0.05$), while they significantly declined in the Rosuvastatin group ($p < 0.05$), suggesting that the hypertensive rat model is successfully established, with significantly increased myocardial function indexes, which can provide important references for early diagnosis.

Cardiac function indexes of rats

In the SHR group, both FS (%) and EF (%) were evidently lower than those in the Control group, while both LVEDd and LVESd were higher than those in

the Control group ($p < 0.05$) (Table 3), indicating that the cardiac functions of hypertensive rats are changed.

Detection results of inflammatory factors in each group

As shown in Table 4, the levels of inflammatory factors TNF- α , IL-6 and MPO were evidently increased in the SHR group compared with those in the other two groups, while they declined in the Rosuvastatin group ($p < 0.05$), suggesting that a large number of inflammatory factors are produced in myocardial tissues in hypertensive rats, which further indicates the development of myocardial injury.

Table 2. Blood pressure and serum biochemical detection results

Group	Systolic blood pressure (mmHg)	Diastolic blood pressure (mmHg)	CK (U/L)	CR (μ mol/L)
Control group	94.9 \pm 2.5	76.9 \pm 3.1	70.1 \pm 1.0	20.7 \pm 0.5
SHR group	158.3 \pm 4.3 ^a	118.5 \pm 5.5 ^a	186.9 \pm 0.8 ^a	85.5 \pm 2.7 ^a
Rosuvastatin group	100.5 \pm 2.7 ^b	85.6 \pm 2.5 ^b	86.6 \pm 0.8 ^b	27.3 \pm 4.5 ^b

Note: Both systolic blood pressure and diastolic blood pressure in the SHR group are significantly higher than those in the Control group ($p < 0.05$). The levels of serum CR and CK are significantly higher in the SHR group than those in the Control group ($p < 0.05$), while they significantly decline in the Rosuvastatin group ($p < 0.05$). ^a $p < 0.05$ vs. Control group, ^b $p < 0.05$ vs. SHR group

Table 3. Cardiac function indexes of rats

Group	LVEDd (mm)	LVESd (mm)	EF (%)	FS (%)
Control group	4.08 \pm 0.85	4.38 \pm 0.29	68 \pm 3.4	58.7 \pm 3.4
SHR group	9.95 \pm 0.55 ^a	7.91 \pm 0.76 ^a	42 \pm 3.6 ^a	36.8 \pm 2.4 ^a
Rosuvastatin group	5.84 \pm 0.27 ^b	5.29 \pm 0.19 ^b	60 \pm 2.7 ^b	52.6 \pm 1.1 ^b

Note: In the SHR group, both FS (%) and EF (%) are lower than those in the Control group, while both LVEDd and LVESd are higher than those in the Control group ($p < 0.05$). ^a $p < 0.05$ vs. Control group, ^b $p < 0.05$ vs. SHR group

Table 4. Inflammatory levels of TNF- α , IL-6 and MPO in Control, SHR and Rosuvastatin groups

Group	IL-6 (mg/L)	TNF- α (fmol/mL)	MPO (μ mg)
Control group	80.1 \pm 4.2	41.1 \pm 3.3	2.6 \pm 1.2
SHR group	160.5 \pm 5.6 ^a	89.6 \pm 6.3 ^a	14.6 \pm 1.4 ^a
Rosuvastatin group	89.8 \pm 5.04 ^b	50.4 \pm 5.4 ^b	4.8 \pm 1.1 ^b

Note: The levels of TNF- α , IL-6 and MPO are increased in the SHR group, while the decline in the Rosuvastatin group. ^a $p < 0.05$ vs. SHR group, ^b $p < 0.05$ vs. Control group

HE staining

The morphological changes in myocardial tissues in each group were detected using HE staining. As shown in Figure 1, the myocardial cells were arranged disorderly with thickening of muscle fibers and inflammatory cell infiltration in SHR group (A), and the myocardial cells had basically the normal structure

and ordered arrangement with mild pathological changes in Rosuvastatin group (B).

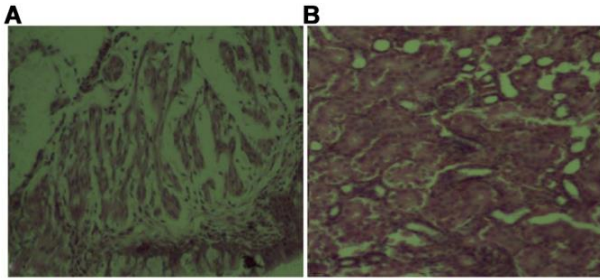


Figure 1. HE staining. The myocardial cells are arranged disorderly with thickening of muscle fibers and inflammatory cell infiltration in the SHR group (A, 10 \times), and the myocardial cells have basically the normal structure and ordered arrangement with mild pathological changes in the Rosuvastatin group (B, 10 \times).

TUNEL staining

The apoptosis level of myocardial tissues was detected using TUNEL staining. As shown in Figure 2, there was almost no myocardial apoptosis in the Control group (A), but a large number of apoptotic myocardial cells were found in the SHR group (B), and myocardial apoptosis declined after rosuvastatin treatment in Rosuvastatin group (C).

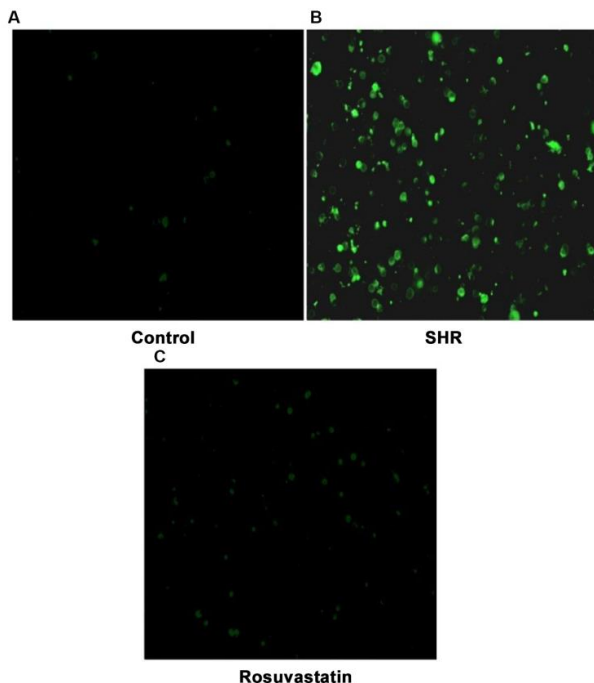


Figure 2. The apoptosis level is detected using TUNEL staining. A large number of apoptotic myocardial cells are found in the SHR group, and myocardial apoptosis declines in the Rosuvastatin group. A: Control group. B: SHR group. C: Rosuvastatin group.

Apoptosis- and pathway-related gene expressions detected using RT-PCR

In the Rosuvastatin group, the Caspase3 and NF- κ B genes were remarkably reduced ($p < 0.05$) and the Bcl-2 and SIRT1 genes were remarkably raised ($p < 0.05$), while these genes showed the opposite trends in the SHR group (Figure 3), demonstrating that myocardial apoptosis is inhibited after rosuvastatin treatment.

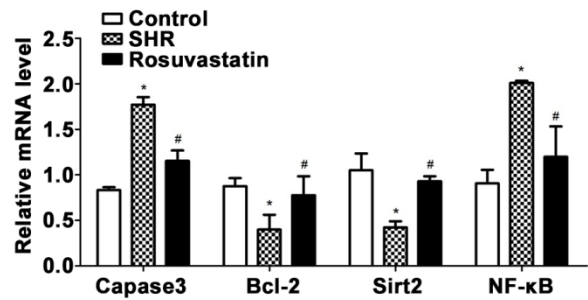


Figure 3. Expression levels of apoptosis- and pathway-related genes. In the Rosuvastatin group, the Caspase3 and NF- κ B genes are remarkably decreased ($p < 0.05$) and the Bcl-2 and SIRT1 genes are remarkably increased ($p < 0.05$), while these genes show the opposite trends in the SHR group. * $p < 0.05$ vs. Control group, # $p < 0.05$ vs. SHR group

Western blotting results

In the Rosuvastatin group, the expression levels of Bcl-2 and SIRT1 were remarkably increased ($p < 0.05$) and the NF- κ B protein expression was remarkably decreased ($p < 0.05$), while the protein expressions in the SHR group showed the opposite trends (Figure 4), indicating that myocardial apoptosis is suppressed after rosuvastatin treatment.

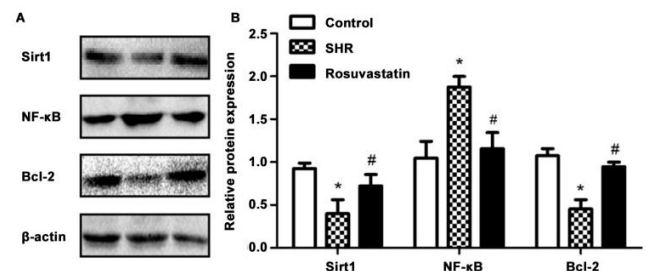


Figure 4. Expression levels of apoptosis- and pathway-related proteins. A: Expression levels of apoptosis- and pathway-related proteins by Western blot. B: Quantification analysis of Western blot result. In the Rosuvastatin group, the expression levels of Bcl-2 and SIRT1 are remarkably increased ($p < 0.05$) and the NF- κ B protein expression is remarkably decreased ($p < 0.05$), while the protein expressions in the SHR group show the opposite trends. * $p < 0.05$ vs. Control group, # $p < 0.05$ vs. SHR group

Both systolic blood pressure and diastolic blood pressure will be significantly increased when hypertension occurs. Hypertension is the most important cause of cardiomyopathy, and human primary hypertension often leads to cardiac remodeling, ventricular hypertrophy and congestive heart failure, and causes cardiac dysfunction, further resulting in severe cardiovascular diseases (16). In the present study, the SHR model was established, and the blood pressure and cardiac function were detected to observe the effect of hypertension on the myocardium. The results showed that both systolic blood pressure and diastolic blood pressure in the SHR group were significantly higher than those in the Control group. According to the detection results of myocardial function indexes, the levels of serum CR and CK were significantly higher in the SHR group than those in the Control group, while they significantly declined in the Rosuvastatin group, suggesting that the hypertensive rat model is successfully established, with significantly increased myocardial function indexes, which can provide important references for early diagnosis. In addition, in SHR group, both FS (%) and EF (%) were lower than those in the Control group, while both LVEDd and LVESd were obviously higher than those in the Control group, indicating that the cardiac functions of hypertensive rats are changed. According to HE staining, the myocardial cells were arranged orderly in the Control group, the myocardial cells were arranged disorderly with thickening of muscle fibers and inflammatory cell infiltration in the SHR group, and the myocardial cells had basically the normal structure and ordered arrangement with mild pathological changes in Rosuvastatin group, demonstrating that hypertension will cause cardiac dysfunction.

Apoptosis plays an important role in maintaining a stable number of myocardial cells, which can remove harmful substances in cells. In the case of lethal threats, the apoptotic reflex will be quickly activated, which, as the defender of the body, supplies energy to the production and metabolism of subcellular structure (17). However, the mechanism of apoptosis in the physiological metabolism of organisms has not been clearly determined. In the present study, the apoptosis level of myocardial tissues was detected using TUNEL staining. It was found that there was almost no myocardial apoptosis in the Control group, but a

large number of apoptotic myocardial cells were found in the SHR group, and myocardial apoptosis obviously declined after rosuvastatin treatment in the Rosuvastatin group. Apoptosis is regulated by apoptosis-related genes and proteins, including Bcl-2 and Caspase3(18). The results of RT-PCR in this study manifested that the Caspase3 expression was remarkably decreased and the Bcl-2 expression was remarkably increased in the Rosuvastatin group, while these gene expressions showed the opposite trends in the SHR group, demonstrating that myocardial apoptosis is inhibited after rosuvastatin treatment, which is consistent with the findings of studies of Qian and Leo et al (19, 20). With the deepening of research on hypertensive cardiomyopathy, the progression of hypertension has been gradually determined, and the clinicopathologic process of hypertension mainly includes the increased cytokines and elevated inflammatory mediators (21), and such inflammatory factors as TNF- α and IL-6 released can activate the downstream key anti-inflammatory transcription factor NF- κ B. As a transcription factor, NF- κ B promotes the production of TNF- α and the expression of inflammatory cytokines (22-24), whereas SIRT1 can inhibit the activation of inflammatory factors and NF- κ B signals (25).

Conclusions

In this study, the levels of inflammatory factors TNF- α , IL-6 and MPO were detected, and it was found that their levels of them were evidently increased in the SHR group compared with those in the other two groups, while they declined in the Rosuvastatin group, suggesting that a large number of inflammatory factors are produced in myocardial tissues in hypertensive rats, which further indicates the development of myocardial injury. Moreover, it was found in gene detection that the NF- κ B expression was remarkably decreased and the SIRT1 expression was remarkably increased in the Rosuvastatin group, while these gene expressions showed the opposite trends in the SHR group. In the SHR group, the NF- κ B protein expression was evidently increased and the SIRT1 protein expression was decreased, suggesting that the activation of the NF- κ B pathway is inhibited and the expression of SIRT1 is promoted after rosuvastatin treatment, thereby benefitting the recovery of myocardial apoptosis in hypertension,

similar to the above study results. To sum up, rosuvastatin can improve myocardial apoptosis in hypertension by activating the SIRT1 pathway and inhibiting the NF- κ B pathway. Despite the conclusion being confirmed, there are still some deficiencies in this experiment. For example, the mechanism of the effect of rosuvastatin on myocardial apoptosis in hypertension was not proved through the cell culture technique. In subsequent studies, therefore, more cell lines can be introduced to explore the specific protective effect of rosuvastatin in myocardial apoptosis using more molecular biological techniques.

In conclusion, rosuvastatin may exert a protective effect against myocardial apoptosis in hypertension, which can alleviate inflammatory cell infiltration and myocardial apoptosis, and such an effect is realized mainly through mediating SIRT1/NF- κ B. The present study provides a theoretical basis for the prevention and treatment of myocardial apoptosis in hypertension and new ideas for subsequent further research as well as research ideas for subsequent development of new drugs.

Acknowledgments

Not applicable.

Interest conflict

The authors declare that they have no conflict of interest.

Funding

No funding was received

Availability of data and materials

The datasets used and/or analyzed during the current study are available from the corresponding author on reasonable request.

Authors' contributions

XR wrote the manuscript. ZR and YW were responsible for the construction of the animal model. LH and ZS performed a TUNEL apoptosis assay and PCR. BY helped with Western blot. All authors read and approved the final manuscript.

Ethics approval and consent to participate

The study was approved by the ethics committee of 940 Hospital of the Joint Service support Force of the Chinese People's Liberation Army.

Consent for publication

Not applicable.

References

1. Kearney PM, Whelton M, Reynolds K, Muntner P, Whelton PK, He J: Global burden of hypertension: analysis of worldwide data. *Lancet* 2005;365: 217-223.
2. Chen HY, Gore JM, Lapane KL, Yarzebski J, Person SD, Gurwitz JH, Kiefe CI, Goldberg RJ: A 35-Year Perspective (1975 to 2009) into the Long-Term Prognosis and Hospital Management of Patients Discharged from the Hospital After a First Acute Myocardial Infarction. *Am J Cardiol* 2015;116: 24-29.
3. Hobbs R, Korutla V, Suzuki Y, Acker M, Vallabhajosyula P: Mechanical circulatory support as a bridge to definitive surgical repair after post-myocardial infarct ventricular septal defect. *J Card Surg* 2015;30: 535-540.
4. Heagerty AM, Heerkens EH, Izzard AS: Small artery structure and function in hypertension. *J Cell Mol Med* 2010;14: 1037-1043.
5. Maghbooli Z, Hossein-Nezhad A: Transcriptome and Molecular Endocrinology Aspects of Epicardial Adipose Tissue in Cardiovascular Diseases: A Systematic Review and Meta-Analysis of Observational Studies. *Biomed Res Int* 2015; 926567.
6. Lavine KJ, Mann DL: Rethinking Phase II Clinical Trial Design in Heart Failure. *Clin Investig (Lond)* 2013;3: 57-68.
7. van Berlo JH, Maillet M, Molkentin JD: Signaling effectors underlying pathologic growth and remodeling of the heart. *J Clin Invest* 2013;123: 37-45.
8. Rohini A, Agrawal N, Koyani CN, Singh R: Molecular targets and regulators of cardiac hypertrophy. *Pharmacol Res* 2010;61: 269-280.
9. Sundstrom J, Lind L, Arnlov J, Zethelius B, Andren B, Lithell HO: Echocardiographic and electrocardiographic diagnoses of left ventricular hypertrophy predict mortality independently of each other in a population of elderly men. *Circulation* 2001;103: 2346-2351.
10. Lai L, Yan L, Gao S, Hu CL, Ge H, Davidow A, Park M, Bravo C, Iwatsubo K, Ishikawa Y, et al: Type 5 adenylyl cyclase increases oxidative stress by transcriptional regulation of manganese superoxide dismutase via the SIRT1/FoxO3a pathway. *Circulation* 2013;127: 1692-1701.
11. Picone P, Giacomazza D, Vetri V, Carrotta R, Militello V, San Biagio PL, Di Carlo M: Insulin-activated Akt rescues Abeta oxidative stress-induced cell death by orchestrating molecular trafficking. *Aging Cell* 2011;10: 832-843.
12. Vallabhapurapu S, Karin M: Regulation and function of NF-kappaB transcription factors in

- the immune system. *Annu Rev Immunol* 2009;27: 693-733.
13. Sierra-Mondragon E, Gomez-Chavez F, Murrieta-Coxca M, Vazquez-Sanchez EA, Martinez-Torres I, Cancino-Diaz ME, Rojas-Espinosa O, Cancino-Diaz JC, Reyes-Sanchez JL, Rodriguez-Munoz R, et al: Low expression of IL-6 and TNF-alpha correlates with the presence of the nuclear regulators of NF-kappaB, IkappaBNS and BCL-3, in the uterus of mice. *Mol Immunol* 2015;68: 333-340.
 14. Ma X, Becker Buscaglia LE, Barker JR, Li Y: MicroRNAs in NF-kappaB signaling. *J Mol Cell Biol* 2011;3: 159-166.
 15. Zhong H, May MJ, Jimi E, Ghosh S: The phosphorylation status of nuclear NF-kappa B determines its association with CBP/p300 or HDAC-1. 2002; *Mol Cell* 9: 625-636.
 16. Zhang WB, Du QJ, Li H, Sun AJ, Qiu ZH, Wu CN, Zhao G, Gong H, Hu K, Zou YZ, et al: The therapeutic effect of rosuvastatin on cardiac remodelling from hypertrophy to fibrosis during the end-stage hypertension in rats. *J Cell Mol Med* 2012;16: 2227-2237.
 17. Klionsky DJ: Autophagy: from phenomenology to molecular understanding in less than a decade. *Nat Rev Mol Cell Biol* 2007;8: 931-937.
 18. Floros KV, Thomadaki H, Florou D, Talieri M, Scorilas A: Alterations in mRNA expression of apoptosis-related genes BCL2, BAX, FAS, caspase-3, and the novel member BCL2L12 after treatment of human leukemic cell line HL60 with the antineoplastic agent etoposide. *Ann N Y AcadSci* 2006;1090: 89-97.
 19. Qian ZQ, Wang YW, Li YL, Li YQ, Ling Z, Yang DL: Icariin prevents hypertension-induced cardiomyocyte apoptosis through the mitochondrial apoptotic pathway. *Biomed Pharmacother* 88: 823-831, 2017.
 20. Jiang FL, Leo S, Wang XG, Li H, Gong LY, Kuang Y and Xu XF: Effect of tanshinone IIA on cardiomyocyte hypertrophy and apoptosis in spontaneously hypertensive rats. *Exp Ther Med* 2013;6: 1517-1521.
 21. Salluh JI, Bozza PT, Bozza FA: Surviving sepsis campaign: a critical reappraisal. *Shock* 30 Suppl 2008;1: 70-72.
 22. Eichacker PQ, Hoffman WD, Farese A, Banks SM, Kuo GC, MacVittie TJ, Natanson C: TNF but not IL-1 in dogs causes lethal lung injury and multiple organ dysfunction similar to human sepsis. *J Appl Physiol* (1985) 71: 1979-1989, 1991.
 23. Connolly MK, Bedrosian AS, Mallen-St Clair J, Mitchell AP, Ibrahim J, Stroud A, Pachter HL, Bar-Sagi D, Frey AB, Miller G: In liver fibrosis, dendritic cells govern hepatic inflammation in mice via TNF-alpha. *J Clin Invest* 2009;119: 3213-3225.
 24. Moosavi, S., Siadat, S., Koochekzadeh, A., Parmoon, G., Kiani, S. Effect of Seed Color and Size on Cardinal Temperatures of Castor Bean (*Ricinus Communis L.*) Seed Germination. *Agrotech Industrial Crops* 2022; 2(1): 1-10. doi: 10.22126/atic.2022.7417.1041
 25. Wang X, Chen L, Peng W: Protective effects of resveratrol on osteoporosis via activation of the SIRT1-NF-kappaB signaling pathway in rats. *Exp Ther Med* 2017; 14: 5032-5038.